Structural Insights into the Interaction between Prion Protein and Nucleic Acid†

Luis Maurício T. R. Lima,‡,§ Yraima Cordeiro,§,||,⊥ Luzineide W. Tinoco,||,# Adriana F. Marques,‡ Cristiano L. P. Oliveira,⊗ Srisailam Sampath,+ Ravindra Kodali,+ Gildon Choi,+ Débora Foguel,⊥ Iris Torriani,⊗ Byron Caughey,+ and Jerson L. Silva*,||,⊥

Faculdade de Farmácia, Centro Nacional de Ressonancia Magnetica Nuclear, Instituto de Bioquímica Médica, and Núcleo de Pesquisa de Produtos Naturais, Universidade Federal do Rio de Janeiro, 21941-590 Rio de Janeiro, RJ Brazil, Instituto de Física "Gleb Wataghin", Unicamp, Campinas, SP 13084-971, Brazil, and Rocky Mountain Laboratories, National Institute of Allergy and Infectious Diseases, Hamilton, Montana 59840

Received March 16, 2006; Revised Manuscript Received May 29, 2006

ABSTRACT: The infectious agent of transmissible spongiform encephalopathies (TSE) is believed to comprise, at least in part, the prion protein (PrP). Other molecules can modulate the conversion of the normal PrP^{C} into the pathological conformer (PrP^{Sc}), but the identity and mechanisms of action of the key physiological factors remain unclear. PrP can bind to nucleic acids with relatively high affinity. Here, we report small-angle X-ray scattering (SAXS) and nuclear magnetic resonance spectroscopy measurements of the tight complex of PrP with an 18 bp DNA sequence. This double-stranded DNA sequence (E2DBS) binds with nanomolar affinity to the full-length recombinant mouse PrP. The SAXS data show that formation of the rPrP−DNA complex leads to larger values of the maximum dimension and radius of gyration. In addition, the SAXS studies reveal that the globular domain of PrP participates importantly in the formation of the complex. The changes in NMR HSQC spectra were clustered in two major regions: one in the disordered portion of the PrP and the other in the globular domain. Although interaction is mediated mainly through the PrP globular domain, the unstructured region is also recruited to the complex. This visualization of the complex provides insight into how oligonucleotides bind to PrP and opens new avenues to the design of compounds against prion diseases.

The cellular PrP (PrP^{C})[1] is constitutively expressed in all mammals (*1*, *2*). The conversion of PrP^{C} into a pathological conformer (PrP^{Sc}) leads to formation of a β-sheet-rich protein at the expense of regions that are flexibly disordered and rich in α-helix (*3*, *4*). This process is promoted by PrP^{Sc} (*5*, *6*) and can be modulated by additional macromolecules (*7*−*13*), in a poorly understood way.

Interaction of PrP with nucleic acids (NA) has been shown to occur both ex vivo (in cellular assays) and in vitro (*9*, *13*−*23*), displaying some sequence (*9*, *23*) and structural (*19*, *20*, *22*, *23*) selectivity. Depending on the conditions of the reaction, the PrP−NA complex may become proteinase K-resistant and undergo amyloid oligomerization (*13*) and conversion to a β-sheet-rich structure (*9*). We have proposed that host nucleic acids may catalyze the conversion between PrP^{C} and PrP^{Sc} by reducing the protein mobility and by making the protein−protein interactions more likely (*9*). Depending on the relative concentration of protein and nucleic acid, binding of DNA to recombinant PrP can promote or inhibit PrP aggregation (*9*, *13*, *14*). Several synthetic nucleic acids increase the level of in vitro PrPres amplification (*13*, *21*). These results are consistent with the hypothesis that endogenous polyanions (such as nucleic acids) may accelerate the rate of prion disease progression by acting as scaffolds or surfaces that facilitate interaction between PrP^{C} and PrP^{Sc} molecules, as previously proposed (*21*). Although all these in vitro experiments suggest that nucleic acids might be active in the PrP^{C} to PrP^{Sc} transition, there is no definitive proof that these molecules may act on the in vivo conversion.

In addition to a still open possibility that nucleic acids (especially from the host) may act on the conversion (*24*), the characterization of a prion protein−nucleic acid complex may be highly relevant for the development of new therapeutic and diagnostic strategies. The recent description that

† This work was supported by grants from Conselho Nacional de Desenvolvimento Científico e Tecnológico (CNPq), Financiadora de Estudos e Projetos (FINEP), Fundação de Amparo à Pesquisa do Estado do Rio de Janeiro (FAPERJ), and Fundação Universitária José Bonifácio (FUJB) of Brazil and by an international grant from the International Centre for Genetic Engineering and Biotechnology (ICGEB) to J.L.S.

* To whom correspondence should be addressed: IBqM, Universidade Federal do Rio de Janeiro (UFRJ), RJ 21941-590, Brazil. Telephone: 55 21 25626756. Fax: 55 21 3881 4155. E-mail: jerson@bioqmed.ufrj.br.

‡ Faculdade de Farmácia, Universidade Federal do Rio de Janeiro.

§ These authors contributed equally to this work.

|| Centro Nacional de Ressonancia Magnetica Nuclear, Universidade Federal do Rio de Janeiro.

⊥ Instituto de Bioquímica Médica, Universidade Federal do Rio de Janeiro.

Núcleo de Pesquisa de Produtos Naturais, Universidade Federal do Rio de Janeiro.

⊗ Unicamp.

+ NIAID.

[1] Abbreviations: PrP, prion protein; Prp^{Sc}, prion scrapie; rPrP, recombinant prion protein; ShaPrP, Syrian hamster prion protein; E2DBS, E2 DNA-binding sequence; SAXS, small-angle X-ray scattering; NMR, nuclear magnetic resonance; NA, nucleic acid; HSQC, heteronuclear single-quantum coherence.

10.1021/bi060532d CCC: $33.50
Published on Web 07/07/2006

degenerate phosphorothioate oligonuclotides (PS-ON) have potent anti-scrapie activities (*22*) highlights the importance of obtaining structural information about PrP−oligonucleotide complexes. The authors have also envisaged the use of PS-ON as prophylactic compounds to be added to blood products prior to transfusion to reduce the risk of TSE transmission (*22*). Takemura et al. (*23*) identified another relevant application of prion−nucleic acid interaction by demonstrating the use of selected DNA aptamers that bind specifically to PrP^{C} for PrP^{Sc} enrichment and as diagnostic tools in double-ligand assay systems. RNA aptamers that bind selectively to disease-associated β-sheet-rich forms of the prion protein have also been isolated (*20*). The authors found that these aptamers inhibit the accumulation of protease-resistant forms of PrP in a prion-seeded, in vitro conversion assay. They suggest the use of synthetic aptamers for the detection of abnormal forms of PrP (*20*).

Another interesting finding was that an anti-DNA antibody could capture PrP^{Sc}, suggesting that PrP^{Sc} forms a complex with nucleic acid (*18*). The authors pointed out the relevance of their results for the development of new strategies for the study, detection, and treatment of prion diseases. All these studies point out the relevance of obtaining structural information about PrP−NA complexes.

Here we describe the first structural characterization of prion protein (PrP) complexed to a small double-stranded oligonucleotide (E2DBS) that we previously found that binds PrP with high affinity (*9*). Although small aptameric RNAs have been shown to bind PrP (*19*, *20*) they are less appropriate for the structural characterization of the complex, because of the much higher degree of complexity and conformational flexibility of ss-RNAs as compared to ds-DNAs. We show how a prion and a NA molecule wrap each other, a picture made possible by the use of two different structural techniques (SAXS and NMR).

EXPERIMENTAL PROCEDURES

Construction, Expression, and Purification of rPrP. $rPrP^{del32-121}$ was obtained as described previously (*25*, *26*). The plasmid for expression of Syrian hamster PrP residues 90−231 ($ShaPrP^{90-231}$) in *Escherichia coli* was created by cloning the DNA coding region for $ShaPrP^{90-231}$ into the Novagen pET23a(+) expression vector. Both rPrPs were expressed and purified as described elsewhere (*9*). To prepare isotopically labeled $ShaPrP^{90-231}$, *E. coli* BL21(DE3) cells harboring the recombinant plasmid were grown in M9 minimal medium supplemented with 0.1% (w/v) ^{15}N-labeled NH_4Cl (99% ^{15}N) and 0.4% (w/v) ^{13}C-labeled glucose (99% ^{13}C). The labeled protein was purified to homogeneity by using nickel affinity chromatography as a principle step according to the procedures reported previously (*27*).

Reagents and Protein Sample. All reagents that were used were analytical grade. NMR measurements were conducted in 20 mM NaAc buffer (pH 5.2), 100 mM NaCl, and 10% D_2O, in the presence or absence of DNA at 30 °C. The synthetic 5′-fluorescein-labeled and unlabeled single-stranded 5′-GTA ACC GAA ATC GGT TGA-3′ (E2DBS) oligonucleotide was purchased from Integrated DNA Technologies (Coralville, IA). Annealing, confirmation of complete hybridization, and determination of its concentration were performed as described elsewhere (*28*).

Fluorescence Spectroscopy. All experiments were performed in 10 mM Tris-HCl (pH 7.4) and 100 mM NaCl, at 22 °C, in an ISS-PC1 spectrofluorimeter (ISS, Champaign, IL) as described previously (*28*). For the anisotropy measurement at pH 5.2 (in 20 mM NaAc buffer and 100 mM NaCl), we used rhodamine-labeled E2DBS. Dissociation constants (K_d) were calculated accordingly (*28*), considering a simple two-state reversible equilibrium between PrP and DNA (PrP + DNA $\rightleftharpoons$ PrP−DNA).

Small-Angle X-ray Scattering Measurements, Data Analysis, and Structural Reconstructions. SAXS data were collected at the D11SAS small-angle scattering beamline of the National Synchrotron Light Laboratory, Campinas, Brazil (*29*), using a one-dimensional position-sensitive detector, with a quartz capillary sample holder and a wavelength λ of 0.1488 nm, at 22 °C. Experiments were conducted in 20 mM Tris, 50 mM NaCl (pH 7.5), and 70 μM DNA. Data acquisition was performed by taking several 600 s frames of each sample. The modulus of scattering vector $\mathbf{q}$ was calculated according to the relation $\mathbf{q} = (4\pi/\lambda) \sin 2\theta$, where λ is the wavelength used and 2θ is the scattering angle. The monodispersity of the samples was confirmed by Guinier plots of the data (*30*) and molecular weight calculations using hen egg lysozyme as a standard (not shown). Data were corrected properly and fitted using GNOM (*30*), and the low-resolution ab initio particle shape was restored using DAMMIN (*31*). Several runs of ab initio shape determination with different starting conditions led to consistent results as judged by the structural similarity of the output models, yielding nearly identical scattering patterns and fitting statistics in a stable and self-consistent process. The final models are a result of an average of five independent calculations, performed using DAMAVER (*32*).

NMR Experiments. The $^{1}H-^{15}N$ HSQC spectra of $ShaPrP^{90-231}$ were assigned as described previously (*33*). The $^{1}H-^{15}N$ and $^{1}H-^{13}C$ HSQC NMR spectra were acquired at 30 °C on a Bruker Avance DRX 600 spectrometer, with 0.18 mM uniformly labeled [^{15}N,^{13}C]$ShaPrP^{90-231}$ in 20 mM sodium acetate buffer (pH 5.2), 100 mM NaCl, and a 10% D_2O/90% H_2O mixture. The sample for the spectra of the $ShaPrP^{90-231}$−DNA complex was prepared by adding 85 μM DNA to the sample of pure $ShaPrP^{90-231}$, and the pH was checked after the addition of DNA. The spectra were processed using NMRPIPE (*34*), and the assignment was performed using NMRVIEW (*35*) based on data from the BMRB4307 star file (*33*).

RESULTS

Small-Angle X-ray Scattering Reveals a Tight Prion−Nucleic Acid Complex. To acquire the structural features of the prion−DNA complex, we used NMR and small-angle X-ray scattering (SAXS). Because of the high concentration of protein and nucleic acid used for both experiments, preliminary experiments were performed to make sure that, at a DNA:PrP concentration ratio of $\geq$1:1, the complex remained soluble. Small-angle X-ray scattering (SAXS) analysis was used to obtain structural information about rPrP and the rPrP−DNA complex. This technique provides direct information about the size, shape, and oligomeric structure of biomolecules in solution. The experimental results for intensity as a function of the modulus of scattering vector $\mathbf{q}$

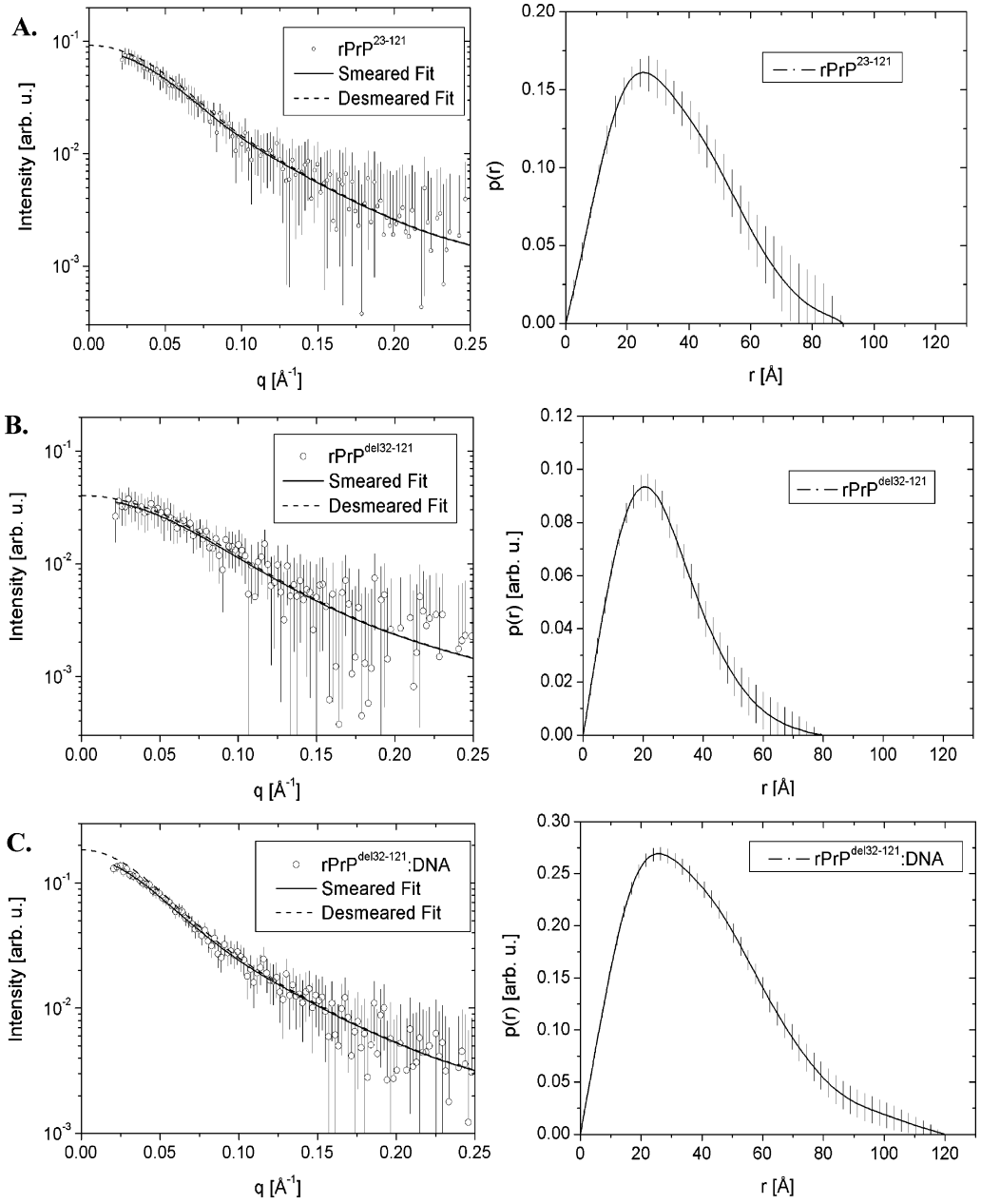

FIGURE 1: Scattered intensity decay obtained by SAXS and pair distance distribution functions calculated from SAXS measurements of (A) free rPrP$^{23-231}$, (B) free rPrP$^{del32-121}$, and (C) the rPrP$^{del32-121}$−DNA complex. The solid line was calculated from the desmeared GNOM fit. Error bars were propagated from the experimental error.

Table 1: Overall Particle Parameters for Free and DNA-Bound rPrP$^{23-231}$ and rPrP$^{del32-121}$ Obtained by SAXS Measurements

PrP construction	anisotropy measurements	SAXS measurements		
	K_d (nM)	DNA	radius of gyration (Å)	maximum distance (Å)
rPrP$^{23-231}$ (pH 7.4)	480 ± 160	−	24 ± 2	90
rPrP$^{del32-121}$ (pH 7.4)	520 ± 220	−	21.2 ± 2	80
rPrP$^{23-231}$ (pH 5.2)	90	+	32 ± 2	120

are shown (Figure 1). We obtained overall dimensional parameters for free rPrP$^{23-231}$ and DNA-bound rPrP$^{del32-121}$ (Table 1). Determination of rPrP$^{23-231}$−DNA complex parameters by SAXS measurements was not possible, since the large oligomers that formed could not be completely removed, probably due to the high concentration required for SAXS measurements.

From the Fourier transformation of the scattering data, we calculated the pair distribution function, $p(r)$, which gives direct information about the particle shape and size. We could observe a characteristic $p(r)$ of a prolate structure (*31*) for both constructs, with the PrP$^{del32-121}$ being less elongated than PrP$^{23-231}$. It is also possible to confirm formation of a complex from the $p(r)$ behavior for the rPrP−DNA complex (Figures 1A−C and 2), which leads to larger values of the corresponding maximum dimension and radius of gyration.

Restoration of ab initio models from SAXS data can give important insight into macromolecular complexes and structural assemblies (*36*). The modeling procedure based on dummy atom models and simulated annealing optimization (*31*) yields a low-resolution three-dimensional model arrangement of a set of spherical beads that gives the best fit of the experimental data. The final low-resolution shapes of

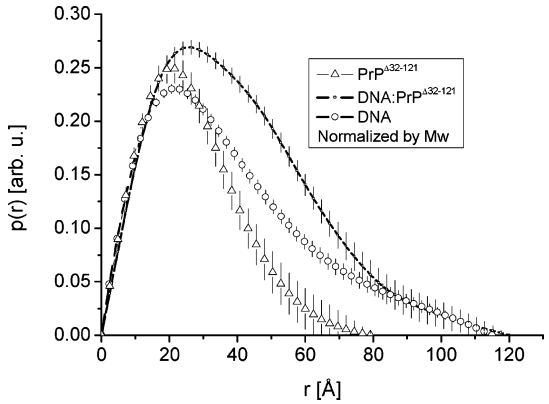

FIGURE 2: Pair distance distribution function calculated from SAXS measurements for free rPrP$^{del32-121}$ (△), the rPrP$^{del32-121}$−DNA complex (- - -), and free DNA (○). Error bars were propagated from the experimental error.

full-length rPrP$^{23-231}$ and the truncated form, rPrP$^{del32-121}$, obtained by modeling from the scattering data indicated an elongated particle, with two distinct domains (Figure 3A). The shape of the molecular models allowed the identification of the globular region of the protein (Figure 3B) as the known murine PrP high-resolution structure (PDB entry 1AG2). In Figure 3C, the rPrP$^{del32-121}$−DNA complex envelope can be visualized. Our results clearly indicate a 1:1 stoichiometry of binding and provide evidence that DNA binding involves the globular domain (Figure 3C).

To further investigate the involvement of the globular domain in nucleic acid recognition, we measured DNA binding affinity for rPrP$^{23-231}$ and for the mutant lacking the N-terminal domain (rPrP$^{del32-121}$). DNA binding was assessed by incubating PrP with fluorescein-labeled DNA and measuring fluorescence anisotropy (*28*). Analysis of equilibrium binding isotherms at pH 7.4 gives apparent dissociation constants of 480 ± 170 nM for rPrP$^{23-231}$ and 525 ± 217 nM for rPrP$^{del32-121}$ (Table 1 and Figure 4A), which are essentially the same within error. DNA binding curves determined at pH 5.2 also show that the full-length prion protein displays high DNA binding affinity (Table 1). At lower salt concentrations (no added NaCl), the affinity was even higher, with a dissociation constant of 30 nM (*9*). This high affinity is close to those of several other DNA-binding proteins, including the E2c DNA-binding protein, which specifically recognizes the DNA employed in this work. The nucleic acid binding of PrP lacking part of the disordered domain confirms the participation of the globular domain (residues 121−231) (*37*) in the formation of a tight complex. However, it does not rule out an influence of the disordered amino acid terminal region in establishing the final DNA-bound conformation.

Protein−nucleic acid interaction is based on many chemical principles, such as electrostatic interaction, van der Waals, hydrophobic, and hydrogen bonding. The apparent affinity in such a type of complex can be modulated by different variables such as temperature and salt concentration. The latter interferes in the electrostatic component of this interaction; i.e., an increase in salt concentration decreases the affinity through a counterion shielding effect over both the protein and NA. An equimolar amount of the PrP−DNA complex was incubated in different concentrations of NaCl, and dissociation was monitored by fluorescence anisotropy of fluorescein-labeled DNA (Figure 4B). The steep dependence of complex dissociation on the NaCl concentration indicates an extensive involvement of electrostatic contacts in DNA recognition by PrP. Other types of chemical interactions are expected to be involved in nucleic acid recognition, which might be revealed by the high-resolution structure of this complex.

NMR Illuminates Amino Acid-Specific Information about the PrP−Oligonucleotide Complex. To further characterize the PrP−DNA complex and map precisely the amino acids that interact with the DNA molecule, we performed nuclear magnetic resonance (NMR) experiments. $^{1}H-^{15}N$ and $^{1}H-^{13}C$ heteronuclear single-quantum coherence (HSQC) spectra were obtained for free and DNA-bound Syrian hamster prion protein (SharPrP$^{90-231}$) in a 90% H_2O/10% D_2O mixture at 30 °C. The HSQC spectra (Figure 5) were assigned on the basis of the published NMR assignment for this construct (*33*). In essence, most of the differences in ^{1}H and ^{15}N chemical shifts between free and DNA-bound ShaPrP$^{90-231}$ samples were small, indicating that the ShaPrP$^{90-231}$ overall fold was maintained. In addition, the minimal chemical shift deviations for most of the $^{13}C^{\alpha}$ and H^{α} resonances confirmed that the overall secondary structure arrangement of the PrP complexed to DNA is similar to that of the free protein. However, we identified substantial changes in localized areas of the protein, with several amino acid residues showing changes in chemical shift values for ^{1}H and ^{15}N equal to or greater than 0.020 ppm (12 Hz) and 0.10 ppm (6 Hz), respectively (Figure 6). These values were on the same order of magnitude as the chemical shift changes observed in the interaction of prion protein with the C-terminal SH3 domain of Grb2 (*38*) and with quinacrine (*39*).

The changes in HSQC were clustered in two major regions: one in the disordered portion of the PrP and the other in the globular domain. Smaller changes were observed in the β-strands and loops (Figure 6A and Table 2). The residues that exhibit the larger modifications are indicated in Table 2.

Except for M213, all large HSQC changes are in amino acids that display universal preferences for interactions between side chains and DNA bases (*40*). The main systematic pattern observed is that most amino acids that display significant changes in HSQC are directed to the same side (Figure 7), which is a typical design of helical DNA-binding motifs.

Taken together, NMR and SAXS data indicate an interaction between the globular domain and DNA. Nevertheless, the NMR data reveal significant changes in the disordered domain, which demonstrate a contribution of this region in the formation of the consolidated complex. Other significant chemical shifts occur in the neighborhood of amino acid residues corresponding to the region where major changes in secondary structure from PrP^{C} to PrP^{Sc} have been reported to occur (*2*). The SharPrP$^{23-231}$ (not shown) and SharPrP$^{90-231}$ uniformly labeled with ^{15}N and ^{13}C show corresponding local changes in chemical shift when bound to DNA, as determined by NMR HSQC spectra (Figure 5). The involvement of structural organization and/or DNA binding by the disordered region of wild-type PrP is suggested by the absence of several peaks corresponding to this portion in the $^{1}H-^{15}N$ HSQC spectra of the ShaPrP$^{90-231}$−DNA

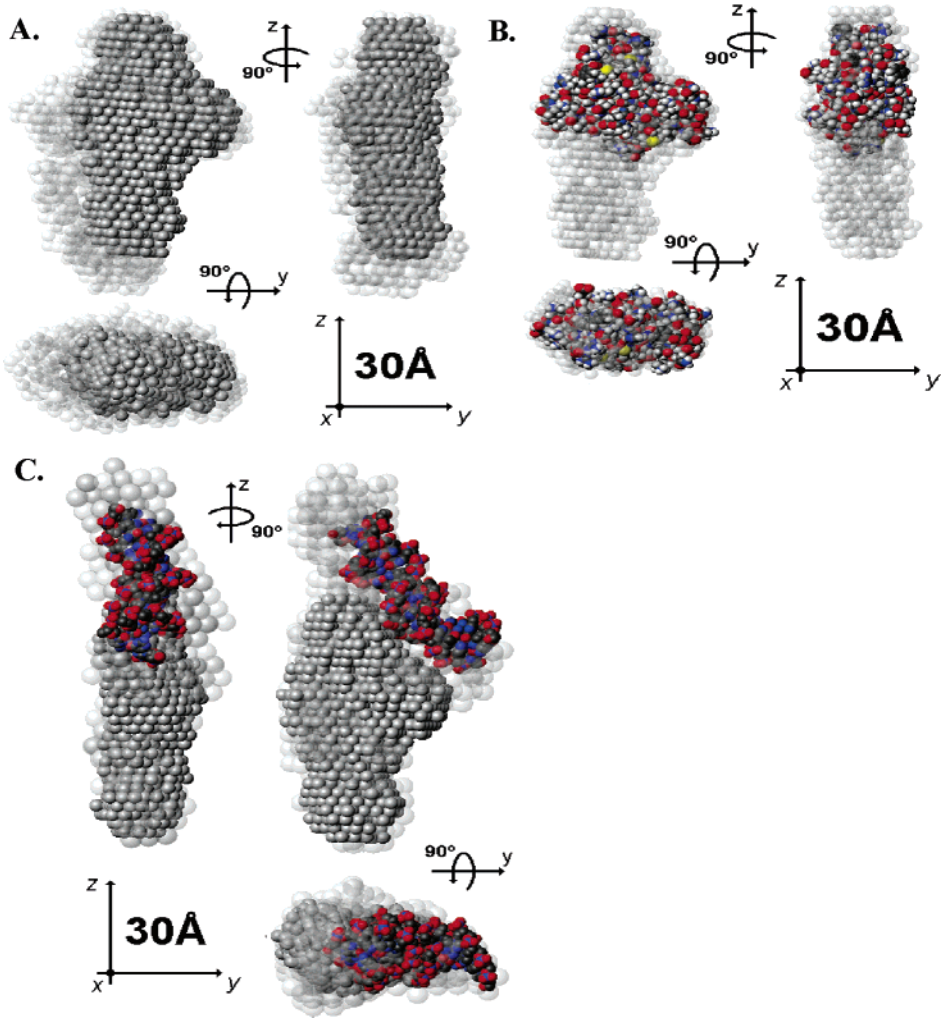

FIGURE 3: Three-dimensional reconstruction of rPrP from SAXS measurements. (A) $rPrP^{23-231}$ (light gray) and $rPrP^{del32-121}$ (dark gray). (B) Superposition of the $rPrP^{del32-121}$ model and the NMR structure of the murine prion protein globular domain (PDB entry 1AG2). (C) $rPrP^{del32-121}$ envelope and crystal structure of a 16 bp DNA (PDB entry 2BOP) superimposed onto the $rPrP^{del32-121}$–DNA complex envelopes. Since the DNA used in this superposition is smaller than the one we used in our measurements and since it is also bent in the crystal structure, complete superposition was not realized.

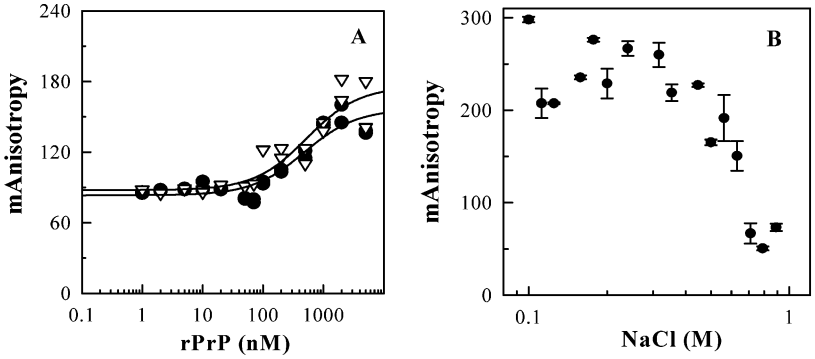

FIGURE 4: Binding of DNA to PrP monitored by fluorescence anisotropy. (A) Free $rPrP^{23-231}$ (black) and $rPrP^{del32-121}$ (white) were assayed for DNA binding at 25 °C for 72 h in 10 mM Tris-HCl with 100 mM NaCl (pH 7.4). (B) Salt dissociation isotherms were determined by incubating 2 μM $rPrP^{23-231}$ with 5 nM F-DNA at 22 °C for 7 days in the presence of varying NaCl concentrations, and the anisotropy was measured.

complex (Figure 5), presumably due to binding-induced peak broadening.

DISCUSSION

Here, we provide the first structural characterization of the prion protein complexed to a nucleic acid, as determined by NMR spectroscopy and SAXS. Prions seem to have other accomplices that chaperone their activity in converting the normal, cellular form into the disease-causing isoform; among chaperone candidates, a nucleic acid is the most likely (*9*, *12*−*17*). The structural identification of a specific site for NA binding will shed light on how PrP interacts with

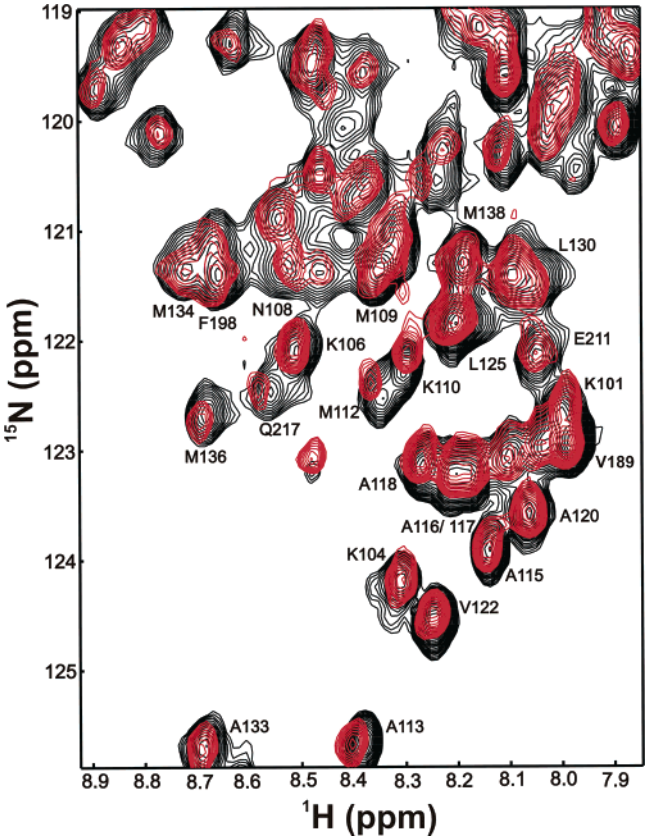

FIGURE 5: ^{1}H−^{15}N HSQC spectra of ShaPrP$^{90-231}$. Expanded region of the superimposed ^{1}H−^{15}N HSQC spectra of free (black) and DNA-bound ShaPrP$^{90-231}$ (red) showing differences in chemical shifts.

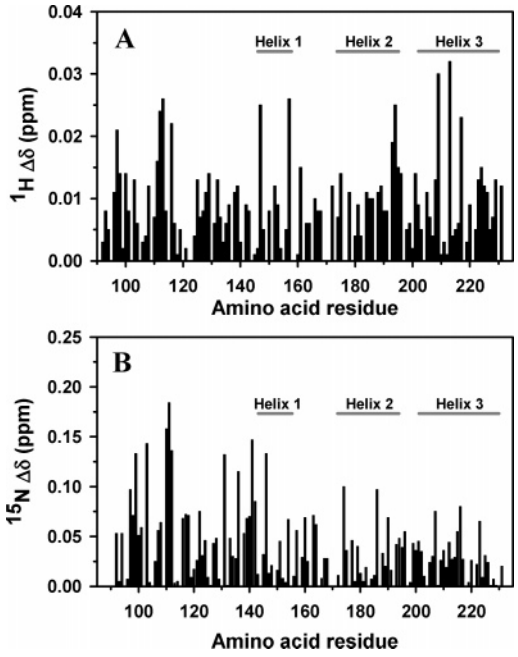

FIGURE 6: Characterization of the ShaPrP structure achieved by DNA binding. Modulus of ^{1}H (A) and ^{15}N (B) chemical shift changes after binding of DNA to ShaPrP$^{90-231}$. The gray bars indicate the position of the Syrian hamster PrP α-helices (*33*).

other molecules, which may affect the conversion to the scrapie conformation. In fact, it has recently been revealed that NAs and other polyanions increase the level of in vitro PrPres amplification (*21*). Because they used purified components, their results are consistent with the hypothesis that endogenous polyanions (such as nucleic acids) may affect the rate of prion disease progression by acting as scaffolds or surfaces that facilitate interaction between PrP^{C} and PrP^{Sc} molecules, as previously proposed (*9*).

Table 2: Amino Acid Changes in Chemical Shift upon Nucleic Acid Binding by PrP

residue[a]	ShaPrP region[b]	^{1}H Δδ (ppm)	residue[a]	ShaPrP region[b]	^{15}N Δδ (ppm)
N97	N-terminus	0.021	W99	N-terminus	−0.133
H111	N-terminus	0.016	S103	N-terminus	0.143
M112	N-terminus	−0.024	K110	N-terminus	0.158
A113	N-terminus	−0.026	H111	N-terminus	0.184
A116	N-terminus	0.022	M112	N-terminus	0.136
D147	helix 1	−0.025	G131	extended strain	−0.132
Y157	loop	−0.026	R136	loop	−0.115
V161	extended strain	−0.015	F141	loop	0.147
T193	helix 2	−0.019	E146	helix 1	−0.133
K194	helix 2	−0.025	N174	helix 2	0.100
G195	loop	−0.015			
V209	helix 3	−0.030			
M213	helix 3	−0.032			
Q217	helix 3	−0.023			
A224	helix 3	−0.015			

[a] The amino acid residues selected in this table were those that displayed chemical shift changes in the ^{1}H−^{15}N HSQC spectrum of DNA-bound ShaPrP$^{90-231}$ of >0.020 and >0.10 ppm for ^{1}H and ^{15}N, respectively. Residues N97, Q98, F141, G142, R151, R156, R164, and Q217 exhibited undersized peaks. Residues N170 and E221 did not exhibit peaks in the ^{1}H−^{15}N HSQC spectrum of DNA-bound ShaPrP$^{90-231}$. [b] Secondary structure assignment of each amino acid residue from ShaPrP$^{90-231}$ (*33*).

The importance of nucleic acid binding by PrP was recently strengthened by the findings that degenerate phosphorothioate oligonucleotides at nanomolar concentrations act as conversion inhibitors with strong anti-scrapie activities in vivo (*22*). The maximum activity was obtained with oligonucleotides with 20−30 bases, consistent with our results which show that oligonucleotide interaction is sterically defined (*22*). Another potential application of DNA binding is in the diagnostics of TSEs (*23*). The authors generated a panel of DNA aptamers that bind to recombinant and mammalian PrP^{C} and not to PrP^{Sc}. They also proposed that PrP^{C}-specific aptamers could be applied as therapeutic tools (*23*).

The globular domain of the PrP protein is the binding site of the antimalarial drug quinacrine, as also demonstrated by NMR spectroscopy (*39*). The disordered portion is also intrinsically involved in the β-sheet content resulting from DNA recognition, as observed by circular dichroism (*9*) and the changes in HSQC spectra. This could be explained by the interaction of DNA with an extended form of the rPrP N-terminal region.

It is noteworthy that several residues, which experience significant chemical shift changes, are in the proximity of histidine residues (Table 2). The changes observed in the unstructured portion of prion protein are centered upon the histidine residues that make up the high-affinity metal-binding site of PrP$^{90-231}$ (H96 and H111) (*41*). Also, residues 141 and 157, which experience significant shift changes, and a large number of the undersized peaks observed in the HSQC spectra (residues 97, 98, 141, and 142) are all in the proximity of histidine residues (ShaPrP residues H96 and H140), suggesting the possible involvement of histidines in

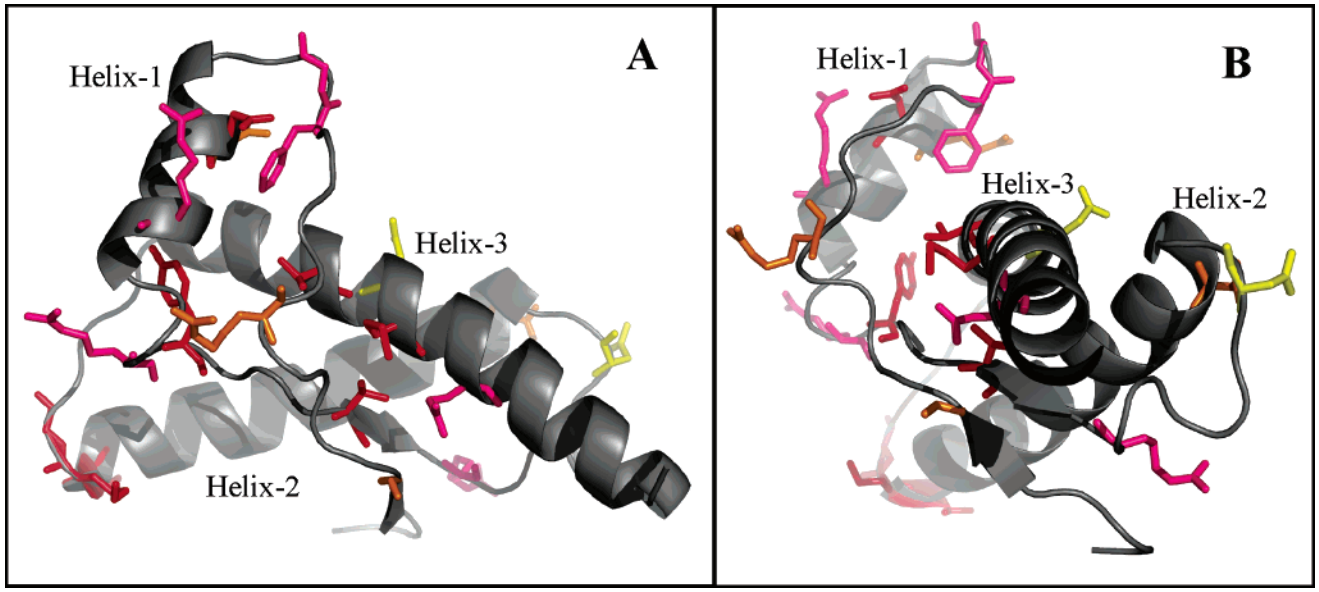

FIGURE 7: (A and B) Ribbon representation of ShaPrP residues L125−G228 (PDB entry 1B10) showing the location of the amino acids that displayed perturbation upon DNA binding: red for residues with >0.02 ppm changes in ^{1}H chemical shift, orange for residues with >0.1 ppm changes in ^{15}N chemical shift, magenta for residues that exhibit undersized peaks, and yellow for residues that do not exhibit peaks.

these effects. However, when the pH is changed from 7.4 to 5.2, there is an only ~5-fold increase in affinity, which indicates that the participation of His residues is important but not crucial for the interaction.

Binding of PrP protein to a nucleic acid molecule is expected to occur with a substantial decrease in the level of hydration. When DNA binds, the changes in the HSQC spectra were in both polar and nonpolar residues (Table 2 and Figure 7). The globular domain of the prion protein presents a significant number of backbone H bonds that are exposed to solvent molecules, with regions of tightly bound conserved waters as well as regions where the local water is in fast exchange with bulk water (*42*). In fact, we found recently that the cellular rPrP isoform is more hydrated and has a larger solvent accessible surface area than aggregated β-rPrP as measured by pressure perturbation calorimetry (*43*). The role of hydration in the folding stability of PrP and in amyloidogenicity has been supported by molecular dynamics (*42*) and high-pressure studies (*43*, *44*). Binding of nucleic acid would be followed by a decrease in solvent accessible surface area and a decrease in the level of hydration.

The structural identification of a specific site of nucleic acid binding opens new avenues to the design of compounds that may interfere with the conversion to the scrapie conformation. In a recent study, we found that the extent of binding of a small hydrophobic compound, bis-ANS (4,4-dianilino-1,1-binaphthyl-5,5-sulfonate), to full-length rPrP is reduced by the addition of nanomolar concentrations of oligonucleotides, demonstrating that they compete for the same binding site (*16*). We and other groups have also found that RNA oligonuleotides also bind PrP. Some aptameric RNAs bind preferentially to the disease-associated conformations of PrP (*19*). We are currently investigating the structure of PrP−RNA complexes, but the main difficulty arises from the dynamics of RNAs being much higher than those ds-DNA oligonucleotides. The intricate behavior of PrP during nucleic acid binding suggests a masked biological recognition function performed by this protein, despite its known outer cell membrane distribution (*1*). Collected evidence suggests a possible functional role in the transport of NA across the cell milieu, placing prion protein in a class of nucleic acid pattern recognition receptors. The fact that NAs can bind PrP and variably affect its conformation and aggregation state raises the additional possibility that PrP−NA interactions might influence neurodegenerative processes associated with TSE diseases.

ACKNOWLEDGMENT

We thank Thomas Privelic and Fernando Q. Reis for assistance in the SAXS beamline setup, Marshall E. Bloom for constructing and providing the ShaPrP$^{90-231}$ expression vector, and Martha M. Sorenson for careful reading of the manuscript.

REFERENCES

1. Aguzzi, A., and Polymenidou, M. (2004) Mammalian prion biology: One century of evolving concepts, *Cell 116*, 313−327.
2. Prusiner, S. B. (1998) Prions, *Proc. Natl. Acad. Sci. U.S.A. 95*, 13363−13383.
3. Caughey, B. W., Dong, A., Bhat, K. S., Ernst, D., Hayes, S. F., and Caughey, W. S. (1991) Secondary structure analysis of the scrapie-associated protein PrP 27−30 in water by infrared spectroscopy, *Biochemistry 30*, 7672−7680.
4. Pan, K. M., Baldwin, M., Nguyen, J., Gasset, M., Serban, A., Groth, D., Mehlhorn, I., Huang, Z., Fletterick, R. J., Cohen, F. E., and Prusiner, S. B. (1993) Conversion of α-helices into β-sheets features in the formation of the scrapie prion proteins, *Proc. Natl. Acad. Sci. U.S.A. 90*, 10962−10966.
5. Kocisko, D. A., Come, J. H., Priola, S. A., Chesebro, B., Raymond, G. J., Lansbury, P. T., and Caughey, B. (1994) Cell-free formation of protease-resistant prion protein, *Nature 370*, 471−474.
6. Saborio, G. P., Permanne, B., and Soto, C. (2001) Sensitive detection of pathological prion protein by cyclic amplification of protein misfolding, *Nature 411*, 810−813.
7. Caughey, B., and Raymond, G. J. (1993) Sulfated polyanion inhibition of scrapie-associated PrP accumulation in cultured cells, *J. Virol. 67*, 643−650.
8. DebBurman, S. K., Raymond, G. J., Caughey, B., and Lindquist, S. (1997) Chaperone-supervised conversion of prion protein to

its protease-resistant form, *Proc. Natl. Acad. Sci. U.S.A. 94*, 13938−13943.
9. Cordeiro, Y., Machado, F., Juliano, L., Juliano, M. A., Brentani, R. R., Foguel, D., and Silva, J. L. (2001) DNA converts cellular prion protein into the β-sheet conformation and inhibits prion peptide aggregation, *J. Biol. Chem. 276*, 49400−49409.
10. Wong, C., Xiong, L. W., Horiuchi, M., Raymond, L., Wehrly, K., Chesebro, B., and Caughey, B. (2001) Sulfated glycans and elevated temperature stimulate PrP(Sc)-dependent cell-free formation of protease-resistant prion protein, *EMBO J. 20*, 377−386.
11. Ben-Zaken, O., Tzaban, S., Tal, Y., Horonchik, L., Esko, J. D., Vlodavsky, I., and Taraboulos, A. (2003) Cellular heparan sulfate participates in the metabolism of prions, *J. Biol. Chem. 278*, 40041−40049.
12. Caughey, B., and Kocisko, D. A. (2003) Prion diseases: A nucleic-acid accomplice? *Nature 425*, 673−674.
13. Deleault, N. R., Lucassen, R. W., and Supattapone, S. (2003) RNA molecules stimulate prion protein conversion, *Nature 425*, 717−720.
14. Gabus, C., Derrington, E., Leblanc, P., Chnaiderman, J., Dormont, D., Swietnicki, W., Morillas, M., Surewicz, W. K., Marc, D., Nandi, P., and Darlix, J. L. (2001) The prion protein has RNA binding and chaperoning properties characteristic of nucleocapsid protein NCP7 of HIV-1, *J. Biol. Chem. 276*, 19301−19309.
15. Nandi, P. K., Leclerc, E., Nicole, J. C., and Takahashi, M. (2002) DNA-induced partial unfolding of prion protein leads to its polymerisation to amyloid, *J. Mol. Biol. 322*, 153−161.
16. Cordeiro, Y., Lima, L. M., Gomes, M. P., Foguel, D., and Silva, J. L. (2004) Modulation of prion protein oligomerization, aggregation, and β-sheet conversion by 4,4′-dianilino-1,1′-binaphthyl-5,5′-sulfonate (bis-ANS), *J. Biol. Chem. 279*, 5346−5352.
17. Mange, A., Crozet, C., Lehmann, S., and Beranger, F. (2004) Scrapie-like prion protein is translocated to the nuclei of infected cells independently of proteasome inhibition and interacts with chromatin, *J. Cell Sci. 117*, 2411−2416.
18. Zou, W. Q., Zheng, J., Gray, D. M., Gambetti, P., and Chen, S. G. (2004) Antibody to DNA detects scrapie but not normal prion protein, *Proc. Natl. Acad. Sci. U.S.A. 101*, 1380−1385.
19. Rhie, A., Kirby, L., Sayer, N., Wellesley, R., Disterer, P., Sylvester, I., Gill, A., Hope, J., James, W., and Tahiri-Alaoui, A. (2003) Characterization of 2′-fluoro-RNA aptamers that bind preferentially to disease-associated conformations of prion protein and inhibit conversion, *J. Biol. Chem. 278*, 39697−39705.
20. Sayer, N. M., Cubin, M., Rhie, A., Bullock, M., Tahiri-Alaoui, A., and James, W. (2004) Structural determinants of conformationally selective, prion-binding aptamers, *J. Biol. Chem. 279*, 13102−13109.
21. Deleault, N. R., Geoghegan, J. C., Nishina, K., Kascsak, R., Williamson, R. A., and Supattapone, S. (2005) Protease-resistant prion protein amplification reconstituted with partially purified substrates and synthetic polyanions, *J. Biol. Chem. 280*, 26873−26879.
22. Kocisko, D. A., Vaillant, A., Lee, K. S., Arnold, K. M., Bertholet, N., Race, R. E., Olsen, E. A., Juteau, J. M., and Caughey, B. (2006) Potent antiscrapie activities of degenerate phosphorothioate oligonucleotides, *Antimicrob. Agents Chemother. 50*, 1034−1044.
23. Takemura, K., Wang, P., Vorberg, I., Surewicz, W., Priola, S. A., Kanthasamy, A., Pottathil, R., Chen, S. G., and Sreevatsan, S. (2006) DNA aptamers that bind to PrP(C) and not PrP(Sc) show sequence and structure specificity, *Exp. Biol. Med. 231*, 204−214.
24. Zou, W. Q., and Gambetti, P. (2005) From microbes to prions the final proof of the prion hypothesis, *Cell 121*, 155−157.
25. Lee, K. S., Magalhaes, A. C., Zanata, S. M., Brentani, R. R., Martins, V. R., and Prado, M. A. (2001) Internalization of mammalian fluorescent cellular prion protein and N-terminal deletion mutants in living cells, *J. Neurochem. 79*, 79−87.
26. Cordeiro, Y., Kraineva, J., Gomes, M. P. B., Lopes, M. H., Martins, V. R., Lima, L. M. T. R., Foguel, D., Winter, R., and Silva, J. L. (2005) The amino-terminal PrP domain is crucial to modulate prion misfolding and aggregation, *Biophys. J. 89*, 2667−2676.
27. Speare, J. O., Rush, T. S., Bloom, M. E., and Caughey, B. (2003) The role of helix 1 aspartates and salt bridges in the stability and conversion of prion protein, *J. Biol. Chem. 278*, 12522−12529.
28. Lima, L. M., and Silva, J. L. (2004) Positive contribution of hydration on DNA binding by E2c protein from papillomavirus, *J. Biol. Chem. 279*, 47968−47974.
29. Kellermann, G., Vicentin, E., Tamura, E., Rocha, M., Barbosa, A. L., Craievich, A., and Torriani, I. (1997) The small-angle X-ray scattering beamline of the Brazilian Synchrotron Light Laboratory, *J. Appl. Crystallogr. 30*, 880−883.
30. Svergun, D. I. (1991) Mathematical methods in small-angle scattering data analysis, *J. Appl. Crystallogr. 24*, 485−492.
31. Svergun, D. I. (1999) Restoring low-resolution structure of biological macromolecules from solution scattering using simulated annealing, *Biophys. J. 76*, 2879−2886.
32. Volkov, V. V., and Svergun, D. I. (2003) Uniqueness of *ab initio* shape determination in small-angle scattering, *J. Appl. Crystallogr. 36*, 860−864.
33. James, T. L., Liu, H., Ulyanov, N. B., Farr-Jones, S., Zhang, H., Donne, D. G., Kaneko, K., Groth, D., Mehlhorn, I., Prusiner, S. B., and Cohen, F. E. (1997) Solution structure of a 142-residue recombinant prion protein corresponding to the infectious fragment of the scrapie isoform, *Proc. Natl. Acad. Sci. U.S.A. 94*, 10086−10091.
34. Delaglio, F., Grzesiek, S., Vuister, G. W., Zhu, G., Pfeifer, J., and Bax, A. (1995) NMRPIPE: A multidimensional spectral processing system based on Unix pipes, *J. Biomol. NMR 6*, 277−293.
35. Johnson, A., and Blevins, R. A. (1994) NMRView: A computer program for the visualization and analysis of NMR data, *J. Biomol. NMR 4*, 603−614.
36. Vachette, P., Koch, M. H., and Svergun, D. I. (2003) Looking behind the beamstop: X-ray solution scattering studies of structure and conformational changes of biological macromolecules, *Methods Enzymol. 374*, 584−615.
37. Riek, R., Hornemann, S., Wider, G., Billeter, M., Glockshuber, R., and Wüthrich, K. (1996) NMR structure of the mouse prion protein domain PrP(121−321), *Nature 382*, 180−182.
38. Lysek, D. A., and Wüthrich, K. (2004) Prion protein interaction with the C-terminal SH3 domain of Grb2 studied using NMR and optical spectroscopy, *Biochemistry 43*, 10393−10399.
39. Vogtherr, M., Grimme, S., Elshorst, B., Jacobs, D. M., Fiebig, K., Griesinger, C., and Zahn, R. (2003) Antimalarial drug quinacrine binds to C-terminal helix of cellular prion protein, *J. Med. Chem. 46*, 3563−3564.
40. Luscombe, N. M., Laskowski, R. A., and Thornton, J. M. (2001) Amino acid−base interactions: A three-dimensional analysis of protein-DNA interactions at an atomic level, *Nucleic Acids Res. 29*, 2860−2874.
41. Jackson, G. S., Murray, I., Hosszu, L. L., Gibbs, N., Waltho, J. P., Clarke, A. R., and Collinge, J. (2001) Location and properties of metal-binding sites on the human prion protein, *Proc. Natl. Acad. Sci. U.S.A. 98*, 8531−8535.
42. De Simone, A., Dodson, G. G., Verma, C. S., Zagari, A., and Fraternali, F. (2005) Prion and water: Tight and dynamical hydration sites have a key role in structural stability, *Proc. Natl. Acad. Sci. U.S.A. 102*, 7535−7540.
43. Cordeiro, Y., Kraineva, J., Ravindra, R., Lima, L. M. T. R., Gomes, M. P. B., Foguel, D., Winter, R., and Silva, J. L. (2004) Hydration and packing effects on prion folding and β-sheet conversion. High-pressure spectroscopy and pressure perturbation calorimetry studies, *J. Biol. Chem. 279*, 32354−32359.
44. Torrent, J., Alvarez-Martinez, M. T., Heitz, F., Liautard, J. P., Balny, C., and Lange, R. (2003) Alternative prion structural changes revealed by high pressure, *Biochemistry 42*, 1318−1325.

BI060532D